

Phase explosion and particle generation phenomena during high power nanosecond laser ablation of silicon

(나노초 레이저 어블레이션에 의한 실리콘의 폭발적 보일링 현상 및 입자발생)

광주과학기술원 기전공학과 정성호

University of California at Berkeley, J. H. Yoo, R. Greif

Lawrence Berkeley National Laboratory, R. E. Russo

I. INTRODUCTION

There have been extensive studies of pulsed laser ablation processes for applications to manufacturing, microfabrication of electronics, thin film deposition, solid sampling for chemical analysis, etc. For laser ablation of solids with nanosecond pulses, the sample undergoes a rapid heating that leads to desorption of mass from the sample by thermal and non-thermal processes. The mass may be removed in the form of vapor, particulates, or solid flakes, resulting in the formation of an ablation crater in the sample. The amount of ablated mass and its form influences the results of most applications; the amount and form of the removed mass depends upon the ablation mechanisms during laser-materials interaction and for high power laser ablation more than a single mechanism may be responsible for the material removal.

When a crystalline silicon was irradiated with a high-power single laser pulse, the ablation crater depth increases first linearly with increasing laser irradiance, then when it reaches a threshold value the crater depth jumps almost four or five times (Fig.1). Beyond the threshold irradiance, $\sim 2.2 \times 10^{10}$ W/cm², the crater depth again increases linearly with laser irradiance. The craters for Fig. 1 were produced on polished silicon samples utilizing a Nd-YAG laser with wavelength and pulse duration of 266 nm and 3 ns, respectively, and measured with an interferometric microscope. The laser beam diameter on the sample surface was approximately 50 μ m. For laser irradiances above the threshold value, a violent material ejection from the sample into the surrounding air was observed after about 300-400 ns from the beginning of laser irradiation, Fig. 2. The elapsed time from the beginning of laser irradiation to the beginning of material ejection was measured with photodiodes and a digital oscilloscope. A detailed description of the experimental system can be found in the Ref. 1. From the images in Fig. 2, the ejected material appeared as a mixture of particulates. For laser irradiances below the threshold, no violent material ejection was observed.

The drastic change in crater depth and material ejection across the threshold laser irradiance is considered to be attributed to different crater generation mechanisms. In this work, the ablation mechanisms in both energy regimes are investigated by employing two theoretical models, i.e. thermal evaporation and phase explosion (or

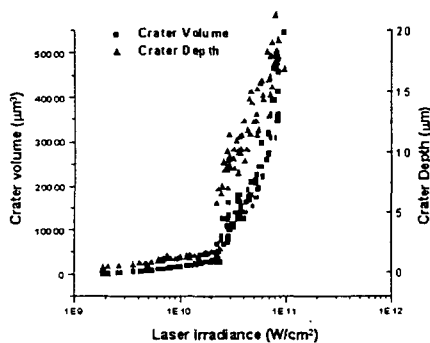


Fig. 1 Variation of measured crater depth and volume as a function of laser irradiance, showing an abrupt increase at 2.2×10^{10} W/cm²

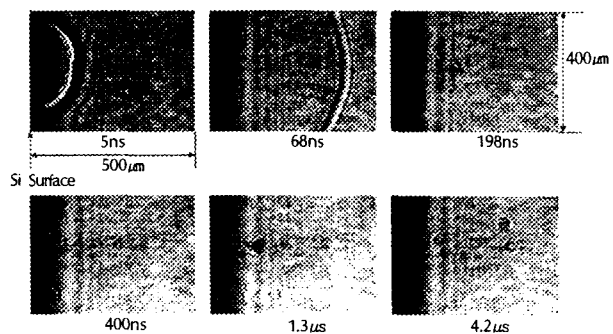


Fig. 2 Mass ejection from the sample at an elapsed time of 400 ns or later for laser irradiance above the threshold. These images were obtained using laser shadowgraphy for laser irradiance of 3.9×10^{10} W/cm²

explosive boiling) for energy regimes below and above the threshold, respectively. For the phase explosion theory, we also employed the theory of induced-transparency of metals near the thermodynamic critical temperature. Ablation depths according to these two laser ablation mechanisms were numerically computed and compared with the experimental data in Fig. 1 and 2.

II. THEORY

Thermal evaporation

Energy conservation for laser heating of solids is represented by the following equation,

$$\rho C \frac{\partial T}{\partial t} - \rho C v \frac{\partial T}{\partial x} = \frac{\partial}{\partial x} \left(k \frac{\partial T}{\partial x} \right) + S \quad (1)$$

where T is temperature, t is time, ρ is density of the sample, C is specific heat, v is the receding velocity of the sample surface during evaporation, and k is thermal conductivity. The spatial coordinate x is in the direction normal to the sample surface with the origin located at the surface. The source term, S , represents the laser energy absorbed by the sample and is expressed as

$$S = I_0(t) \alpha \exp(-\alpha x)$$

where I_0 is the temporal laser power density at the sample surface and α is the absorption coefficient of the sample material at the incident laser wavelength. v in Eq. (1) is represented by

$$v = \dot{m}_v / \rho_l \quad (2)$$

where \dot{m}_v is the mass flux of vapor evaporated from a liquid surface estimated using the Hertz-Knudsen formula²⁾, and ρ_l is the density of the liquid.

To solve Eq. (1), two boundary conditions are required at $x=0$ and $x=L$, where L is the length of the computational domain. At $x=L$, the temperature of the material is assumed to be unaffected during the laser irradiation. At $x=0$, an adiabatic boundary condition, i.e. $\partial T / \partial x = 0$, was used when there is no surface evaporation. When vaporization exists at the surface, the energy loss at this boundary was calculated for the total latent heat of evaporating mass.

Phase explosion of superheated liquid

Phase explosion during laser ablation refers to an abrupt release of material near the thermodynamic critical temperature. Martynyuk conducted pioneering work investigating phase explosion experimentally and theoretically.^{3,4)} He observed violent explosion of a rapidly heated metal wire and attributed this phenomenon to the homogeneous nucleation within a molten metal layer. More recently, Kelly reported the importance of phase explosion in pulsed laser sputtering as a primary mechanism for material removal.⁵⁾

For laser ablation of silicon with a nanosecond pulse, the temperature of liquid silicon near the irradiated surface rapidly increases beyond its equilibrium saturation temperature, causing the liquid silicon to become superheated. When the superheated liquid become unstable, it is said to be reached the spinodal limit. Near the spinodal limit, the superheated liquid experiences an intense fluctuation of density⁶⁾, leading to a homogeneous generation of vapor nuclei in the liquid. This density fluctuation is known to occur at temperatures approximately between 0.8 and $0.85 T_c$ ⁵⁾. The vapor nuclei may either grow to a larger size or collapse in the liquid. Once a vapor bubble grows to a size greater than a critical radius, denoted by r_c , it grows spontaneously. The critical radius and the time for a spherically symmetric bubble in extensive superheated liquid to grow to the critical radius can be expressed as⁶⁾

$$r_c = \frac{2\sigma}{p_{sat}(T_l) \exp\left\{ \nu_l \left[p_l - p_{sat}(T_l) \right] / R_v T_l \right\} - p_l}, \quad \tau_c = r_c \left\{ \frac{2 \left[T_l - T_{sat}(p_l) \right] L_{ev} \rho_v}{3 \left[T_{sat}(p_l) \right] \rho_l} \right\}^{-0.5} \quad (3-1,2)$$

where σ is the surface tension of the liquid, $\nu_l = 1/\rho_l$, R_v is the gas constant of the vapor, and L_{ev} is the latent heat of evaporation. When vapor bubbles with radii greater than r_c are generated homogeneously and steadily in the entire superheated liquid, the superheated liquid undergoes a rapid transition into a mixture of vapor bubbles and equilibrium liquid droplets, leading to a rapid expansion of the mixture, i.e. a phase explosion.

During phase explosion, the expansion of the mixture of high pressure bubbles and liquid droplets into the surrounding air leads to a violent ejection of mass from the sample.

Induced transparency of liquid silicon at near critical temperature

When a metallic sample is heated by intense laser irradiation to near the thermodynamic-critical temperature, the liquid metal becomes almost transparent to the incident laser radiation, by transforming into a liquid dielectric.^{7,8,9)} This phenomenon which occurs due to a strong reduction of electron density in the liquid metal near critical temperature is called induced-transparency or bleaching of liquid metals, and is known to occur at about $0.9T_c$, denoted by T_t . When the temperature of the liquid reaches T_t , the liquid becomes transparent and the incident laser energy penetrates through this transparent layer to the underneath material. Because the liquid below the transparent layer may also reach T_t by subsequent heating, the transparency front propagates into the interior liquid until laser radiation ceases.

III. RESULTS AND DISCUSSION

A laser pulse with a Gaussian energy distribution was used in the calculation. Total pulse duration and pulse width at $1/e$ of the maximum intensity were 6 and 3 ns, respectively, with the maximum located at 3 ns. Laser fluences, F , in the calculation ranges from 10 to 100 J/cm^2 . The spatial domain of 50 or 100 μm (depending upon the laser fluence) was uniformly divided with an individual grid size of 12.5 nm; the variation in calculated results for smaller grid sizes was negligible. Time steps of 0.1 and 1 picosecond were used for the thermal evaporation and the induced-transparency models, respectively. The thermal and optical properties of silicon used in the computation are from Ref.10. The initial temperature of the sample was set equal to 300 K.

The computed thicknesses of the induced-transparency layer and the thermally evaporated layer are shown in Fig. 3 with the measured crater-depth data in Fig. 1 which are replotted for laser fluences.

Thermal evaporation

The receding velocity of the evaporation front, calculated using Eq. (3), is shown in Fig. 4. By integrating this receding velocity with time, the total thickness of the liquid layer removed due to thermal evaporation, denoted by 'evaporation depth', was calculated. Despite the large receding velocity with maximum values ranging from about 100 to 700 m/sec, the computed evaporation depth varied only from about 0.2 to 2.2 μm (cf.

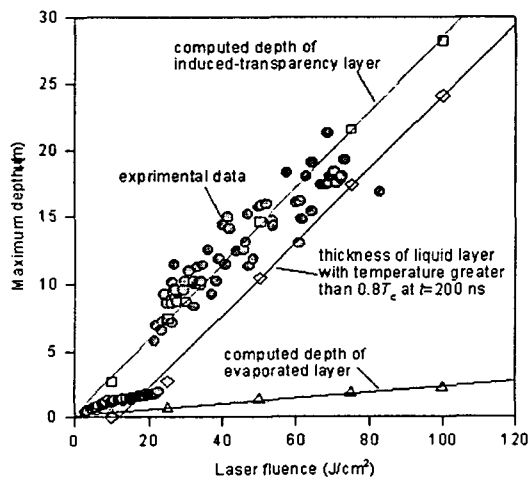


Fig. 3 Comparison of measured crater depth (●) with computed data (□: maximum depth of induced-transparency layer; ◇: thickness of liquid layer with temperature over $0.8T_c$ at $t=200$ nsec; △: evaporation depth)

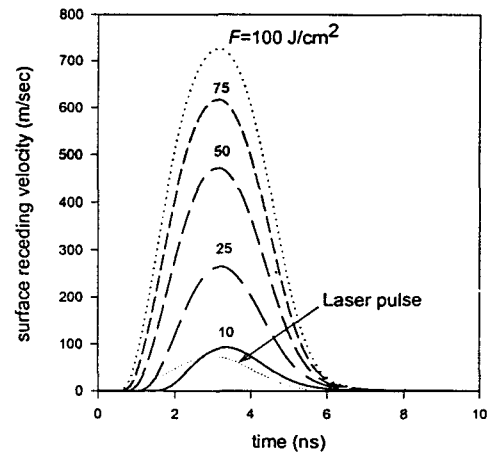


Fig. 4 Receding velocity of the evaporation front with respect to laser pulse energy (Thermal evaporation model)

Fig. 3). The computed evaporation depth in Fig. 3 is approximately one half of the measured crater depth for laser fluences up to about 25 J/cm^2 , at which point the jump in the measured crater depths occurred. For laser fluences above 25 J/cm^2 , the computed evaporation depth is less than the measured crater depth approximately by an order of magnitude.

Phase explosion with induced-transparency

It is assumed that an induced-transparency of liquid silicon occurs when its temperature reaches $0.9T_C$. Because the thermodynamic critical temperature of silicon is unavailable in the literature, we assumed that it lies in the same range as that of common metals like aluminum, copper, zinc, silver etc. for which T_C lies approximately between 3000-6000 K. The effect of the critical temperature on the thickness of computed transparent layer was examined for three different values of T_C , i.e. 5000, 7000, and 9000 K, for a laser fluence of 100 J/cm^2 . The thickness of the maximum transparent layer decreased about 40 % when the critical temperature was increased from 5000 to 9000 K (cf. Fig. 5), demonstrating that the order of magnitude of the transparent layer thickness is not significantly affected by the selected critical temperature.

The computed thickness of the transparency layer in Fig. 3 agrees with the measured crater depths for laser fluences above the threshold value of about 25 J/cm^2 . Furthermore, the agreement in the slopes of the measured crater depth and the computed transparency-layer thickness demonstrates that the induced-transparency of the liquid silicon during laser ablation is a possible process at this energy regime. However, the computed thickness of the induced-transparency layer itself does not represent the measured crater depth. Instead, the transparency layer provides the conditions that may lead to the processes responsible for generating deep craters, that is, phase explosion. For phase explosion to take place, the vapor bubbles produced within the superheated metastable liquid must grow above the critical radius. For liquid silicon at 4150 K (i.e. at $0.83T_C$), the critical radius and the corresponding growth time computed by Eqs. (3-1) and (3-2) are $0.8\text{-}4.0 \text{ }\mu\text{m}$ and $90\text{-}490 \text{ nsec}$, respectively. The critical radius and the corresponding growth time was estimated over a range of probable values because the surface tension of the liquid silicon at high temperature is unknown; decrease of the surface tension with increasing temperature from the value at the melting temperature was considered. Recall that the violent material ejection from the sample was observed after about 300-400 ns from the beginning of laser irradiation (Fig. 2). This time scale is consistent with the estimated bubble growth time.

These time scales, both experimental and theoretical, demonstrate that for a phase explosion to take place, the liquid silicon should maintain the superheated state for at least 100-400 ns to allow bubbles to grow to the

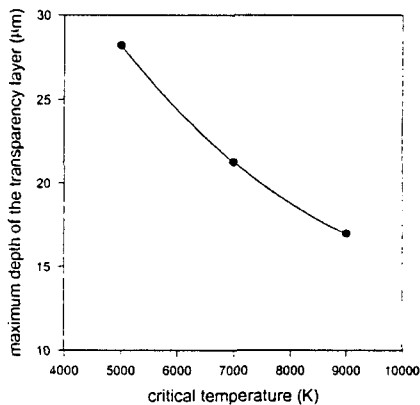


Fig. 5 Variation of the maximum of the computed induced-transparency layer with respect to thermodynamic critical temperature ($F=100 \text{ J/cm}^2$)

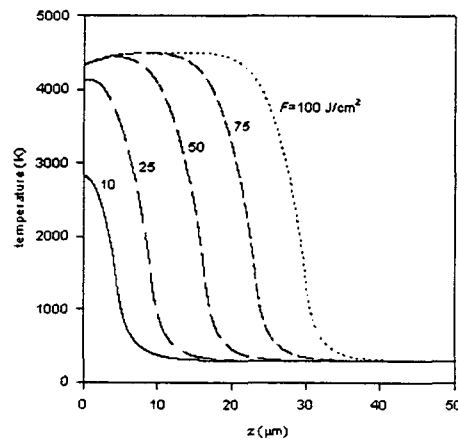


Fig.6 Temperature distribution inside the sample for different laser fluences after 200 nsec from the laser pulse (Induced-transparency model)

critical size. The temperature distribution inside the sample at different times shows that after 600 ns from the beginning of laser irradiation, the thickness of liquid layer at temperatures above $0.8T_C$ is over 20 μm for $F=100 \text{ J/cm}^2$. Therefore, the liquid within 20 μm from the surface has sufficient time to allow vapor bubbles to grow to the critical size. The thickness of the liquid layer with temperatures above $0.8T_C$ at a certain time varies with laser pulse energy (cf. Fig.6). In Fig. 3, the thickness of the induced-transparency layer for $F=10 \text{ J/cm}^2$ was about 2.7 μm . However, after 200 ns, this transparency layer disappears completely as shown in Fig. 6 and no part of the liquid is above $0.8 T_C$, implying that the vapor bubbles would not have enough time to grow to the critical size; no phase explosion would occur in this case. For $F=25 \text{ J/cm}^2$, the thickness of the induced-transparency layer is about 12 μm . For this laser fluence, the thickness of the liquid layer with temperatures above $0.8T_C$ at $t=200 \text{ ns}$ is about 3.0 μm and a phase explosion can occur in this region. The thickness of liquid layer with temperatures above $0.8T_C$ at $t=200 \text{ ns}$ increases linearly with the same slope as the induced-transparency layer thickness and the measured crater depths (cf. Fig. 3). These results demonstrate that for laser ablation with fluences of 25 J/cm^2 or greater, the thickness of the induced-transparency layer is sufficiently large to maintain the temperature of the superheated liquid layer above $0.8T_C$ over 200 ns after the laser irradiation. When this condition is satisfied, the vapor nuclei will grow to the critical size leading to a phase explosion.

IV. CONCLUSION

The nonlinear increase of ablation depth during single pulse laser irradiation was investigated with thermal evaporation and phase explosion modeling. Thermal evaporation is found to significantly underestimate the measured depth and thus inadequate to describe the experimentally obtained data. For laser irradiances above the threshold value, a good agreement is obtained between the measured crater depth and the calculated superheated liquid layer when an induced-transparency of the liquid silicon is introduced. These results support that induced transparency and explosive boiling may play an important role in forming the deep craters.

REFERENCES

1. J. H. Yoo, S. H. Jeong, R. Greif, and R. E. Russo, *Journal of Applied Physics*, Vol. 88., 2000, p.1638
2. S. H. Jeong, R. Greif, and R. E. Russo, *Proceedings of the ASME Heat Transfer Division*, Vol. 351, 1997, p.68
3. M. M. Martynyuk, *Sov. Phys. Tech. Phys.* Vol. 19, No. 6, 1974, pp. 793-797
4. M. M. Martynyuk, *Sov. Phys. Tech. Phys.* Vol. 21, No. 4, 1976, pp. 430-433
5. R. Kelly and A. Miotello, *Applied Surface Science*, Vol. 96-98, 1996, pp. 205-215
6. V. P. Carey, *Liquid-vapor phase change phenomena*, Taylor & Francis, 1992
7. V. A. Batanov, F. V. Bunkin, A. M. Prokhorov, and V. B. Fedorov, *Soviet Physics JETP*, Vol. 36, No. 2, 1973, pp. 311-322
8. R. V. Karapetyan and A. A. Samokhin, *Sov. J. Quant. Electron.*, Vol. 4, No. 9, 1975, pp. 1141-1142
9. F. V. Bunkin and M. I. Tribelskii, *Sov. Phys. Usp.* Vol 23, No. 2, 1980, pp. 105-133
10. Muller, S. De Unamuno, B. Prevot, and P. Dhamelincourt, *Phys. Stat. Sol. (A)*, Vol. 158, 1996, pp. 385-396